

ARTICLE

Investigation of the anticancer mechanism of monensin via apoptosis-related factors in SH-SY5Y neuroblastoma cells

Sema Serter Kocoglu¹  | Ceren Oy²  | Mücahit Secme³  | F. Bahar Sunay¹ 

¹Department of Histology and Embryology, School of Medicine, Balikesir University, Balikesir, Turkey

²Department of Histology and Embryology, School of Medicine, Bursa Uludag University, Bursa, Turkey

³Department of Medical Biology, School of Medicine, Ordu University, Denizli, Turkey

Correspondence

Sema Serter Kocoglu, Department of Histology and Embryology, Faculty of Medicine, Balikesir University, Balikesir 10145, Turkey.

Email: serter_bio@hotmail.com

Funding information

Scientific and Technological Research Council of Turkey, Grant/Award Number: TUBITAK-SBAG-120S399

Abstract

Monensin is an ionophore antibiotic that inhibits the growth of cancer cells. The aim of this study was to investigate the apoptosis-mediated anticarcinogenic effects of monensin in SH-SY5Y neuroblastoma cells. The effects of monensin on cell viability, invasion, migration, and colony formation were determined by XTT, matrigel-chamber, wound healing, and colony formation tests, respectively. The effects of monensin on apoptosis were determined by real-time polymerase chain reaction, TUNEL, Western blot, and Annexin V assay. We have shown that monensin suppresses neuroblastoma cell viability, invasion, migration, and colony formation. Moreover, we reported that monensin inhibits cell viability by triggering apoptosis of neuroblastoma cells. Monensin caused apoptosis by increasing caspase-3, 7, 8, and 9 expressions and decreasing Bax and Bcl-2 expressions in neuroblastoma cells. In Annexin V results, the rates of apoptotic cells were found to be $9.66 \pm 0.01\%$ ($p < 0.001$), $29.28 \pm 0.88\%$ ($p < 0.01$), and $62.55 \pm 2.36\%$ ($p < 0.01$) in the 8, 16, and $32 \mu\text{M}$ monensin groups, respectively. In TUNEL results, these values were, respectively; $35 \pm 2\%$ ($p < 0.001$), $34 \pm 0.57\%$ ($p < 0.001$), and $75 \pm 2.51\%$ ($p < 0.001$). Our results suggest that monensin may be a safe and effective therapeutic candidate for treating pediatric neuroblastoma.

Study Highlights

WHAT IS THE CURRENT KNOWLEDGE ON THE TOPIC?

Neuroblastoma is the most common extracranial childhood tumor originating from neural crest cells. Neuroblastomas constitute ~15% of childhood cancer deaths. There is a need to develop new and alternative advanced treatment approaches for neuroblastoma oncogenesis. Monensin is an ionophore antibiotic with antiparasitic and antibacterial effects.

WHAT QUESTION DID THIS STUDY ADDRESS?

No study has been found on the anticancer properties of monensin on neuroblastoma cell proliferation, migration, invasion, and apoptosis. This study addresses dose-dependent and apoptotic pathway-mediated anticarcinogenic properties of monensin in neuroblastoma cells in vitro.

WHAT DOES THIS STUDY ADD TO OUR KNOWLEDGE?

Monensin suppresses neuroblastoma cell proliferation, invasion, migration, and colony formation. Monensin triggers apoptosis by increasing caspase-3, 7, 8, 9, and cleaved-PARP1 expressions and decreasing Bax and Bcl-2 expressions.

HOW MIGHT THIS CHANGE CLINICAL PHARMACOLOGY OR TRANSLATIONAL SCIENCE?

Monensin may be a safe and effective therapeutic drug candidate in the treatment of pediatric neuroblastoma.

INTRODUCTION

Neuroblastoma is the most common extracranial childhood tumor originating from neural crest cells.¹ Neuroblastomas are the most common solid tumors in infants. In children and adolescents, they are the most common solid tumors after brain tumors. Neuroblastomas constitute ~15% of childhood cancer deaths.²⁻⁵ About 90% of the patients are under the age of 5 years, and most of them are newborns and babies because it is a tumor that occurs predominantly in the embryological period.^{6,7} Neuroblastoma most commonly begins in the adrenal gland tissue, as an abdominal mass, and has a heterogeneous phenotype. Children younger than 18 months present with metastases to the liver, skin, and bone marrow (stage MS disease), but this may resolve spontaneously (without treatment). In children older than 18 months (stage M disease), it is associated with an aggressive clinical phenotype and poor survival. Children over 18 months of age with stage M disease and/or MYCN amplification are clinically classified as having high-risk neuroblastoma.⁸

In treating pediatric neuroblastoma, chemotherapy, radiotherapy, surgery, immunotherapy, and gene therapy are applied depending on the patient's physiological condition, structure, localization, and tumor stage.^{6,9}

Despite improving the methods used to treat the disease, the survival rate remains below 40%. Therefore, the lack of desired results with surgery and other treatment approaches in neuroblastoma, a tumor originating from the nervous system, has led to the need to develop new and alternative advanced treatment approaches to neuroblastoma oncogenesis.^{10,11}

Natural polyether antibiotics arouse interest due to their antifungal, antiparasitic, antibacterial, and antiviral properties. The polyether backbone of these compounds can form complexes with metal cations and transport them across lipid cell membranes. As a result, this event disrupts the natural cation balance in the lipid cell membrane and initiates apoptosis. Recent studies have shown that polyether ionophores may be important chemotherapeutic agents that can overcome cancer stem cells and multidrug resistance and act in various types of cancer.¹²

Monensin is an ionophore antibiotic obtained from "*Streptomyces cinnamonensis*" with known antibacterial and antiparasitic effects and provides Na⁺/H⁺ ion exchange in cell membranes.¹³ Monensin has been accepted by the US Food and Drug Administration as a growth promotor in cattle and poultry.¹⁴ It was observed that the usage of monensin increased milk production in cattle without causing any side effects in terms of animal health. It has been shown to reduce the mitochondrial transmembrane potential, suppress the cell cycle, inhibit protein secretion, and be a potent inducer of oxidative stress in renal cell carcinoma and other cell lines. Recent studies with different types of cancer, such as prostate,¹⁵ lung,¹⁶ pancreatic,¹⁷ and breast cancer¹⁸ have shown that this antibiotic has highly effective and exciting anticancer properties.

No study has been found in the literature showing the anticancer properties of monensin mediated by apoptosis in neuroblastoma cells in vitro. The aim of this study was to investigate the apoptosis-mediated anticarcinogenic effects of monensin in SH-SY5Y neuroblastoma cells.

MATERIALS AND METHODS

Cell culture

The human neuroblastoma SH-SY5Y (ATCC:CRL-2266) cell line was used in this study. Cells were incubated at 37°C under 95% air and 5% CO₂ pressure in DMEMF12 (Dulbecco's Modified Eagle Medium) culture medium containing penicillin (20 units/mL), streptomycin (20 µg/mL), and 10% fetal bovine serum (FBS). Monensin (Abcam) was dissolved in ethanol and its concentration was arranged as less than 0.5%. SH-SY5Y cells were dose and time-dependently incubated with 8, 16, 32, and 64 µM monensin for 24, 48, and 72 h.

Colorimetric XTT method

The cytotoxic effect of monensin on SH-SY5Y cells was determined by the colorimetric XTT method. SH-SY5Y

cells (1×10^4 cells/well) were seeded in 96-well plates and incubated for 24 h. Control and monensin dose groups (8, 16, 32, and 64 μM) were formed and incubated in a 5% CO_2 incubator for 24, 48, and 72 h. All experiments were performed in three replicates. At the end of each incubation period, the XTT (Biotium) assay was applied according to recommendation of the manufacturer. Formazan formation was measured spectrophotometrically at 450 nm (630 nm wavelength reference) using a microplate reader (Thermo Scientific). The absorbance difference was calculated by subtracting the value measured at 630 nm from the value measured at 450 nm. The ratio between the absorbance difference and control group absorbance, the percent mortality, and half-maximal inhibitory concentration (IC_{50}) values were calculated. The effect of monensin on the viability of SH-SY5Y neuroblastoma cells and the IC_{50} value were calculated using XTT and AAT bioquest online tool.

$$\% \text{Cell viability} = \frac{450 \text{ nm optical density} - 630 \text{ nm optical density}}{\text{Control optical density value}} \times 100.$$

Invasion

Invasion activities of the control and dose groups were investigated with the “transwell matrigel invasion chamber.”

The invasion well was placed in a medium containing FBS, and SH-SY5Y cells were plated in serum-free DMEM/F12 on the matrigel membrane of 2.5×10^5 cells/well. Control and monensin dose groups (8, 16, and 32 μM) were formed and incubated for 48 h. At the end of the incubation, the cells remaining without invasion in the invasion well were cleaned with the help of a sterile and clean swab. To identify invading cells, the cells were fixed with cold methanol for 10 min and stained with crystal violet dye for 3 min. The remaining dye in the invasion well was removed with the help of sterile and clean ear sticks. The number of invaded cells was counted under the light microscope in five randomly selected areas at $40\times$ magnification, and the number of invaded cells was calculated.

$$\text{Invasion \%} = \frac{\text{Number of cells in matrix basement membrane}}{\text{Number of cells in control membrane}}$$

Wound healing test

Wound healing assay was performed to evaluate the effects of monensin on the migration of SH-SY5Y cells. Cells were seeded in 12-well plates at 2.5×10^5 cells/well density. When the cells reached 90% density, a straight line was drawn on the bottom of the plates with a sterile 200 μL pipette tip, and control and dose groups (8, 16,

and 32 μM monensin) were formed and incubated at 37°C and 5% CO_2 , for 48 h. Cells were photographed at 0, 16, and 24 h to show cell migration in the control and dose groups. Wound healing was evaluated in three repetitions, and wound distances were calculated using the Image J program.

Colony evaluation

To determine how monensin affects colony formation in SH-SY5Y neuroblastoma cells, 10^3 cells/well were seeded in six-well culture plates for the control and dose groups. After the cells adhered to the bottom of the well, DMEM/F-12 was applied to the control group, and monensin doses (8, 16, and 32 μM) were applied to the dose group; all cells were incubated for 48 h. After incubation, the control and dose groups media were removed, and new DMEM/F-12 media were added to both groups. After this stage, the media of the control and dose groups were changed every 2 days, and this process was continued for 14 days. Colonies were fixed with cold methanol and stained with crystal violet for 15 min. The stained colonies were counted under an inverted microscope, and the difference between the dose and control groups was calculated.

TUNEL assay

SH-SY5Y cells were seeded in eight-well plates at a density of 10×10^3 cells/well. After 24 h of incubation at 37°C , control and dose groups (8, 16, and 32 μM) were formed and incubated for 48 h at 37°C under 5% CO_2 pressure. Subsequently, they were washed with phosphate-buffered saline (PBS) and fixed with 4% paraformaldehyde. TUNEL assay was done with the Roche In Situ Cell Death Detection Kit, as recommended by the manufacturer. Imaging was performed under a fluorescent microscope, and “percent” apoptosis was found by comparing viable cells to apoptotic cells at $40\times$ magnification in at least 10 randomly selected areas from the control and dose groups.

Annexin V evaluation

To determine the apoptotic effects of monensin on SH-SY5Y cells, cells were seeded in six-well plates at a density of 5×10^5 cells/well. After incubation, control and dose groups (8, 16, and 32 μM) were formed and incubated for 48 h at 37°C , 5% CO_2 pressure. After incubation, cells were collected and centrifuged at 2000g for 5 min. Subsequently, cells were washed two times with cold PBS and stained with Annexin V and Dead Cell Assay Kit for

at least 30 min at room temperature. Cells were analyzed using the Muse Cell Analyzer (Millipore).

Real-time polymerase chain reaction

SH-SY5Y cells were seeded in six-well plates at 3×10^5 cells/well density and incubated at 37°C for 24 h. In the follow-up, control and monensin doses (8, 16, and 32 μM) were applied and incubated for 48 h. Total RNA was isolated according to the trizol reagent protocol. The cDNA synthesis was performed with the Transcriptor High Fidelity cDNA Synthesis Kit (abm, cat. no: G904) according to the manufacturer's instructions.

The mRNA-level expressions of the genes involved in the apoptosis pathway from the obtained cDNAs were analyzed in a real-time polymerase chain reaction (RT-PCR) device (Applied-Biosystems) using the SYBR Green method. To determine gene expressions, gene expressions were normalized using the housekeeping gene GAPDH. Fold changes of gene expressions were calculated, and experiments were repeated three times. Forward and reverse sequences of apoptosis-related genes investigated in this study are given in [Table S1](#).

Western blot

In order to evaluate apoptosis at the protein level, SH-SY5Y cells were seeded in 75 cm² flasks. After 24 h of incubation at 37°C, control and dose groups (8, 16, and 32 μM) were formed and incubated for 48 h. Protein isolation was performed on ice using RIPA lysis buffer containing protease and phosphatase inhibitors. Concentrations of proteins were determined according to the kit procedure using the BCA kit (ABP Biosciences). Proteins were separated using 12% SDS/PAGE (20 μg) and transferred to PVDF membrane (EMD Millipore). The PVDF membrane was blocked with 5% milk powder (Bioshop, cat. no: SKI400.500) and incubated with primary antibodies overnight at +4°C. After 24 h of incubation, anti-rabbit horseradish was incubated with peroxidase-conjugated secondary antibodies (1:20,000, cat. no. BT-AS00010, BTLab) for 1 h at room temperature. Proteins were found with the WesternBright ECL HRP substrate kit (Advansta) and visualized using a digital scanner (C-Digit Blot Scanner; Licor Biosciences). Anti-Bax (1:1000, cat. no. BT-AP00842, BTLab), anti-Bcl (1:1000, cat. no. BT-AP00858, BTLab), anti-Caspase-3 (1:1000, cat. no. BT-AP01203, BTLab), anti-Caspase-7 (1:1000, cat. no. BT-AP01207, BTLab), anti-Caspase-8 (1:1000, cat. no. BT-AP01209, BTLab), anti-Caspase-9 (1:1000, cat. no. BT-AP01215, BTLab), anti-cleaved-PARP1 (1:1000, cat. no. BT-AP01959, BTLab), and anti-beta actin (1:5000, cat. no.

BT-AP09788, BTLab) were purchased from BTLab Bioassay Technology.

Statistical analysis

Data analysis was quantitated with a computer program using the $\Delta\Delta C_T$ method for RT-PCR analysis. Volcano Plot analyses, available in the web-based RT² Profiler PCR Array Data Analysis program, were used. SPSS 23 analysis was performed for the other experiments. Comparison of the groups was evaluated statistically by the Student *t*-test analysis and/or Tukey or Tamhane in One Way ANOVA follow-up, and $p < 0.05$ was considered significant.

RESULTS

Monensin inhibits SH-SY5Y neuroblastoma cell viability

In the presented study, it was shown that monensin decreases SH-SY5Y cell viability in a dose- and time-dependent manner.

We have not found a dose at which monensin reduces SH-SY5Y cell viability to 50% at 24 h. In 24 h groups, 8, 16, 32, and 64 μM monensin decreased cell viability only to 83%, 67%, 57%, and 60%, respectively ([Figure 1](#)).

In 48 h, 8, 16, 32, and 64 μM monensin decreased cell viability up to 59%, 48%, 29%, and 30%, respectively. The IC₅₀ dose of monensin in SH-SY5Y cells at 48 h was determined as 16 μM ([Figure 1](#)). The 16, 8, and 32 μM , the lower and upper dose groups, were determined as the doses to be applied during the following experiments ([Figure 1](#)).

In 72 h, 8 μM monensin reduced SH-SY5Y cell viability to 47%. The 16 μM monensin decreased cell viability to 48%, 32 μM to 45%, and 64 μM to 40%. Because the results

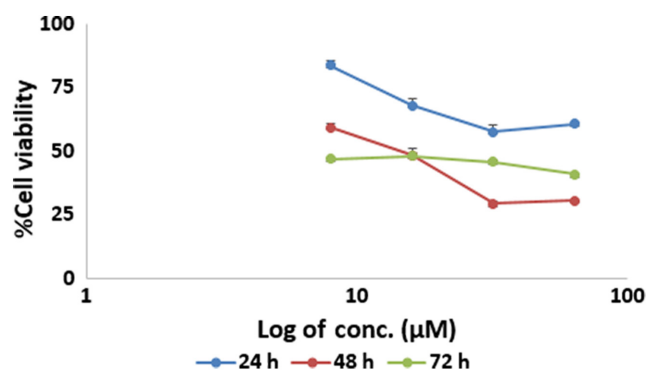


FIGURE 1 Cytotoxic effects of monensin on SH-SY5Y cells. The half-maximal inhibitory concentration dose of monensin in SH-SY5Y cells at 48 h was determined as 16 μM .

of 48 h of monensin application to SH-SY5Y cells were more significant and the monensin administration time was shorter, 48 h of administration was preferred during the following experiments (Figure 1).

Our results suggest that monensin may be an agent that can reduce neuroblastoma cell viability.

Monensin suppresses SH-SY5Y neuroblastoma cell colony formation, migration, and invasion

The number of SH-SY5Y cell colonies was significantly decreased in the groups treated with monensin compared

to the control group ($p < 0.001$; Figure 2). Although the number of colonies was 101 ± 2.08 in the control group, it was found as 7 ± 2.51 , 3 ± 1.15 , and 0 ± 0.00 in the groups treated with 8, 16, and $32 \mu\text{M}$ monensin, respectively (Figure 2b). Compared to the control group, the rate of decrease in the number of colonies was 93%, 97%, and 100% in the groups treated with 8, 16, and $32 \mu\text{M}$ monensin, respectively.

Monensin administration caused a decrease in the invasion capacity of SH-SY5Y cells (compared with the control group, $p < 0.001$; Figure 3). Whereas the number of invading cells in the 8, 16, and $32 \mu\text{M}$ monensin groups was 308 ± 20 , 178 ± 5 , and 123 ± 4 , respectively, this number was 633 ± 27 in the control group (Figure 3b).

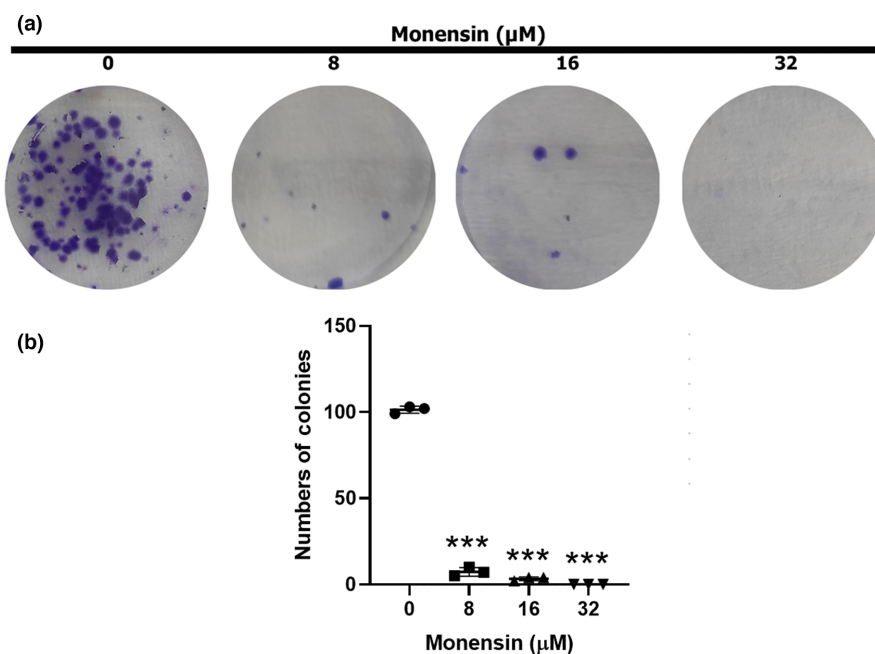


FIGURE 2 Monensin reduces colony formation of SH-SY5Y cells. (a) Sample images of colony formation after 48 h in groups treated with 0, 8, 16, and $32 \mu\text{M}$ monensin. (b) Colony numbers decreased significantly in monensin applied groups compared to the control group. Data are presented as mean \pm SD, $n = 3$, *** $p < 0.001$.

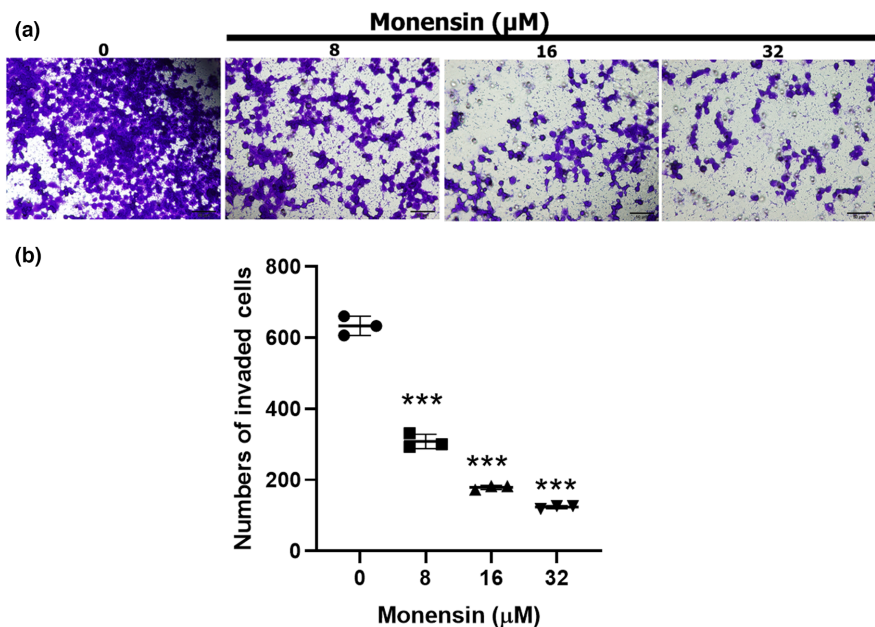


FIGURE 3 Monensin reduces the invasion of SH-SY5Y cells. (a) Sample images of cells that invaded after 48 h in groups treated with 0, 8, 16, and $32 \mu\text{M}$ monensin. (b) Number of cells showing invasion in the groups treated with 0, 8, 16, and $32 \mu\text{M}$ monensin. Data are presented as mean \pm SD, $n = 3$, *** $p < 0.001$.

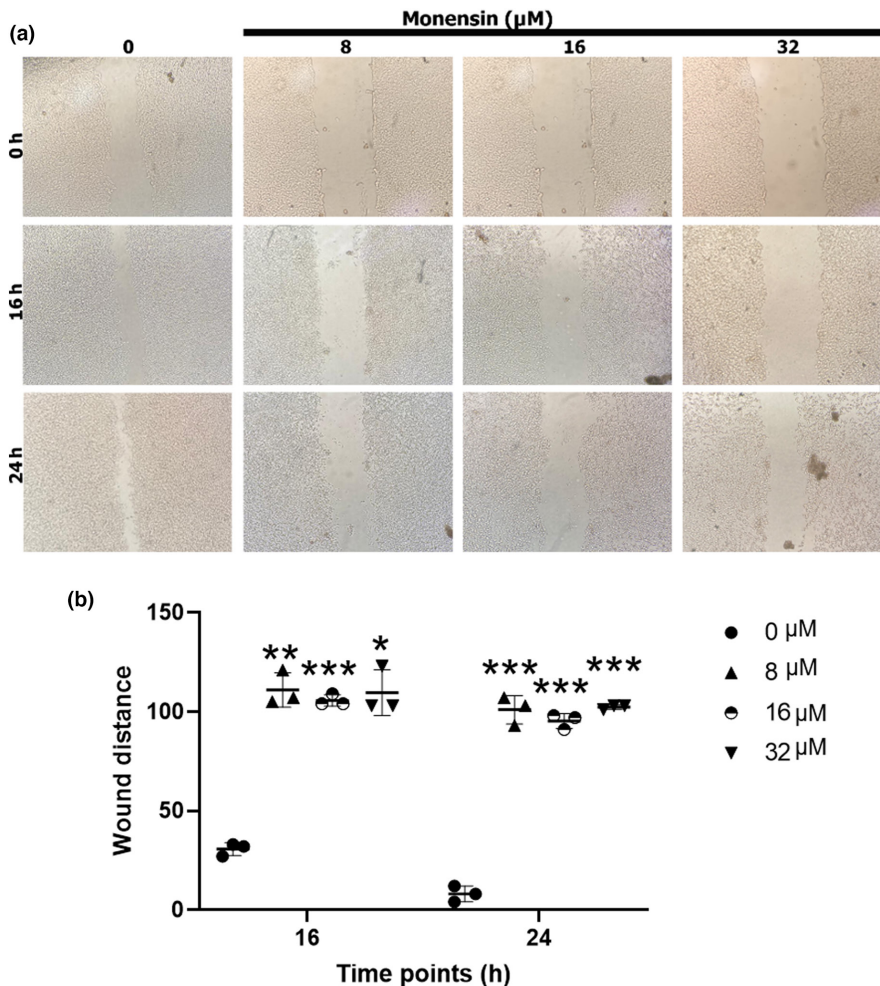


FIGURE 4 Monensin reduces the migration of SH-SY5Y cells. (a) Wound healing images at 0, 16, and 24 h in groups treated with 0, 8, 16, and 32 μM monensin. (b) Relative wound distances at 0, 16, and 24 h in groups treated with 0, 8, 16, and 32 μM monensin. Data are presented as mean ± SD, $n = 3$, $*p < 0.05$, $**p < 0.01$, $***p < 0.001$.

Compared to the control group, 8 μM monensin reduced the invasion of SH-SY5Y cells by 51%, 16 μM monensin by 71%, and 32 μM monensin by 80%.

Monensin administration significantly decreased the migration of SH-SY5Y cells compared to the control group ($p < 0.001$; Figure 4). Wound distances at 16 h in control, 8, 16, and 32 μM monensin groups were 30 ± 3.21 , 111 ± 8.71 ($p < 0.001$), 105 ± 2.88 ($p < 0.001$), and 109 ± 11 ($p < 0.001$), respectively (Figure 4b). At 24 h, these values were 8 ± 4 , 101 ± 7.21 ($p < 0.001$), 95 ± 3.78 ($p < 0.001$), and 102 ± 1.15 ($p < 0.001$), respectively (Figure 4b). Cell migration decreased in the groups treated with monensin at 16 and 24 h compared to the control group (Figure 4a).

Our results suggest that monensin administration may be an agent that can reduce SH-SY5Y cell invasion, migration, and colony formation.

Monensin promotes SH-SY5Y neuroblastoma cell apoptosis

To answer the question of how monensin reduces cell viability in SH-SY5Y cells, the apoptosis-mediated effects of

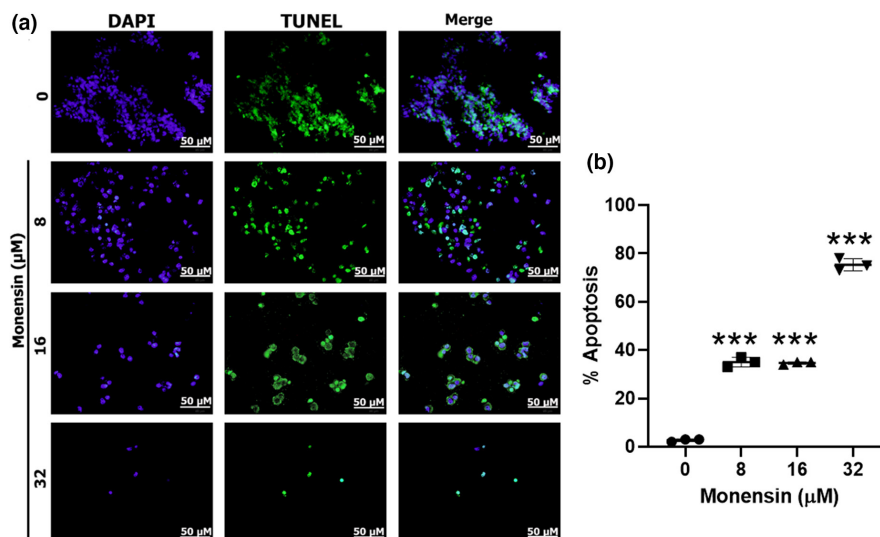
monensin in SH-SY5Y cells were investigated by TUNEL, Annexin V, RT-PCR, and Western blot methods.

In the TUNEL evaluation, it was shown that monensin significantly increased the apoptosis of SH-SY5Y cells compared to the control group ($p < 0.001$; Figure 5). Although the rate of apoptotic cells in the control group was $2.66\% \pm 0.57\%$, in the groups administered 8, 16, and 32 μM monensin, it was $35 \pm 2\%$ ($p < 0.001$), 34 ± 0.57 ($p < 0.001$), and 75 ± 2.51 ($p < 0.001$), respectively (Figure 5b).

The Annexin V method confirmed that monensin induced apoptosis of SH-SY5Y cells (Figure 6). Whereas the rate of apoptotic SH-SY5Y in groups monensin applied at 8, 16, and 32 μM for 48 h, was $9.66 \pm 0.01\%$ ($p < 0.001$), $29.28 \pm 0.88\%$ ($p < 0.01$), and $62.55 \pm 2.36\%$ ($p < 0.01$), respectively, in the control group it was $0.57 \pm 0.02\%$ (Figure 6e).

RT-PCR analyses showed significant changes in the mRNA levels of some apoptosis-related genes in SH-SY5Y cells treated with 8, 16, and 32 μM monensin (Table S2). Application of 8 μM monensin triggered apoptosis in SH-SY5Y cells by increasing caspase-3, caspase-7, DR5, BMF, and BAD expressions, and decreasing caspase-9 expression. The application of 16 μM

FIGURE 5 Evaluation of the effects of monensin on apoptosis in SH-SY5Y cells by TUNEL. The left column after 48 h is DAPI (+); the middle column is TUNEL (+); the right column is the merged sample fluorescent microscope images. (b) Quantitative evaluation of the tunnel signal. Data are presented as mean \pm SD, $n = 3$, *** $p < 0.001$.



monensin significantly increased the expression levels of caspase-7, MCL1, NOXA, BIRC3, BCLAF, and BMF (Table S2). Application of 16 μM monensin induced apoptosis by increasing the expression levels of caspase-3, NOXA, and decreasing the expression level of caspase-9 (Table S2).

Western blot results showed that the protein levels of genes associated with apoptosis were changed in monensin-treated SH-SY5Y cells compared to the control group (Figure 7). 8, 16, and 32 μM monensin triggered apoptosis by reducing Bax and Bcl-2 expressions. 8 μM monensin induced apoptosis by increasing the expression levels of caspase-7, 8, and 9. It has been reported that 16 and 32 μM monensin triggered apoptosis by increasing caspase-3, 7, 8, and 9, and cleaved-PARP1 expressions (Figure 7). Our results suggest that monensin triggers apoptosis of SH-SY5Y cells by increasing the expression of caspase-3, 7, 8, and 9, and cleaved-PARP1 and decreasing the expression of Bax and Bcl-2.

DISCUSSION

Neuroblastoma is an early childhood tumor with heterogeneous biological, morphological, genetic, and clinical characteristics associated with the sympathetic nervous system.¹⁹ Neuroblastomas have a very poor prognosis in children over 18 months of age, with metastasis to the liver, bone marrow, skin, and other organs.¹⁹ Even in treatment protocols with intensive chemotherapy, radiation, surgery, and hematopoietic stem cell transplantation, the survival rate is around 40%–50%.²⁰ Although progressive studies are conducted to understand neuroblastomas' biological and molecular mechanisms, the disease still accounts for 15% of childhood deaths. As a result, new therapeutic targets are needed to treat the disease.^{5,21}

The advances in molecular studies and the gradual elucidation of some of the mechanisms that control the metastasis, division, and development of tumor cells have led researchers to discover new therapeutic agents that are less toxic in cancer therapy, do not damage healthy tissues and organs, and are less costly. Monensin is an oil-soluble natural bioactive ionophore obtained from *Streptomyces cinnamonensis*. Monensin exchanges Na^+ and K^+ ions across the cell membrane, causing disruption of ion gradients and altering cell physiology. It causes deterioration of pH stability in the cell and accumulation of calcium in the cells. As a result, mitochondrial damage, cell swelling, and cell cavitation in the cell lead to decreased cell proliferation and apoptosis.^{14,18,22} The US Food and Drug Administration approves monensin for use in veterinary medicine. However, it exerts a broad spectrum of activity against human pathogens in drug-susceptible and resistant strains.²² The anticancer activity of monensin in different cancer cells has been demonstrated in previous studies. In the present study, dose-dependent and apoptotic pathway-mediated anticarcinogenic properties of monensin in neuroblastoma cells were investigated for the first time.

Monensin has been shown to dose-dependently reduce UOK146 renal cancer cell proliferation.²³ Another study reported that monensin inhibited PC-3 and LNCaP prostate cancer cell growth.²⁴ It has been shown to inhibit the Wnt signaling pathway in colorectal cancer and suppress the development of multiple intestinal tumors.^{14,23} Monensin has been shown to suppress tumor growth and proliferation through the EGFR signaling pathway in drug-resistant pancreatic cancer cells.¹⁷ In our study, monensin was shown to decrease SH-SY5Y neuroblastoma cell viability in a dose and time-dependent manner. The IC_{50} dose of monensin in SH-SY5Y neuroblastoma cells was determined as 16 μM .

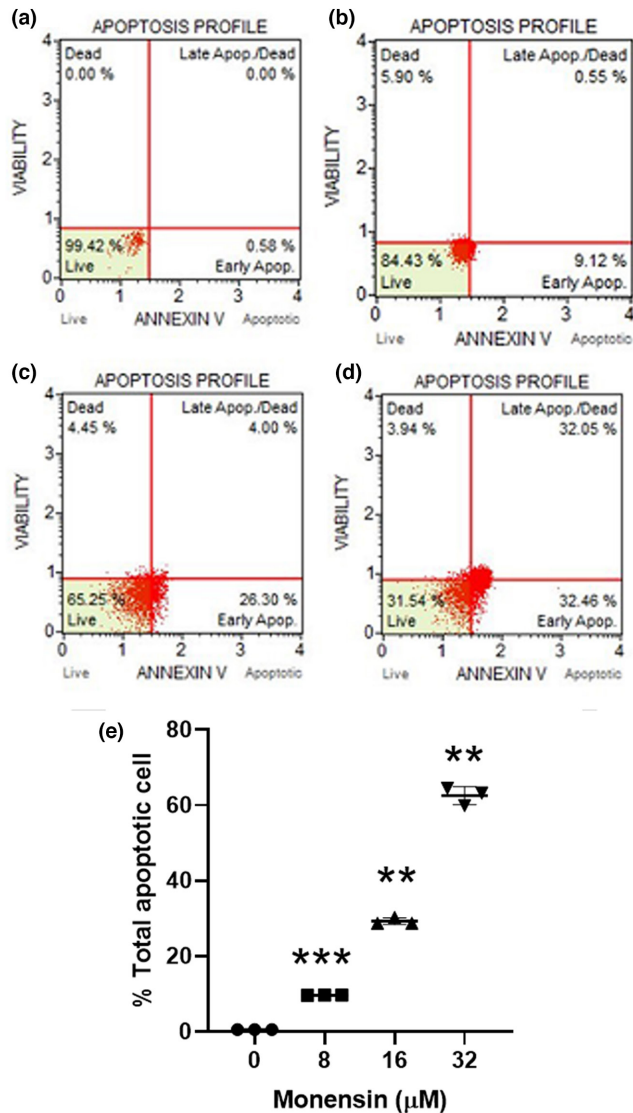


FIGURE 6 Evaluation of the effects of monensin on apoptosis in SH-SY5Y cells by Annexin V staining. Apoptosis profile obtained after 48 h of treatment with (a) control, (b) 8, (c) 16, (d) 32 μM monensin. (e) Statistical comparison of total apoptotic cells in SH-SY5Y cells (** $p < 0.01$ and *** $p < 0.001$).

Gu et al. showed that monensin reduces cell migration and invasion and activates apoptosis in breast cancer cells.¹⁸ In another study, it was shown that migration and wound healing decreased in Panc-1 and MiaPaCa-2 pancreatic cancer cells treated with monensin.¹⁷ In the presented study, we showed for the first time that monensin significantly reduced invasion, migration, and colony formation of SH-SY5Y cells in a dose- and time-dependent manner. The 8 μM monensin reduced the invasion of SH-SY5Y cells by 51%, 16 μM monensin by 71%, and 32 μM monensin by 80%. Monensin administration significantly decreased the migration of SH-SY5Y cells at 16 and 24 h compared to the control group ($p < 0.001$). The rate of decrease in the number of colonies was 93%, 97%, and 100% in the groups treated with

8, 16, and 32 μM monensin, respectively. Our results clearly show that monensin reduces neuroblastoma cells' invasion, migration, and colony formation.

The safe background profile of monensin in animal systems provides an advantage for elucidating its molecular mechanisms. Kim et al.²⁴ reported that monensin activates caspase-3 and causes apoptosis by increasing intracellular calcium changes and reactive oxygen species production. Park et al.²⁵ reported that monensin suppresses the growth of human lymphoma cells mediated by apoptosis.

It has been reported that monensin inhibits the androgen signaling pathway, causing apoptosis and oxidative stress, especially in prostate cancer cells.¹⁵ Again, in lung cancer cells, 50 nM concentration of monensin has been shown to increase apoptosis induced by rapamycin (mTOR inhibitor) and erlotinib (EGFR inhibitor).¹⁶ Gu et al.¹⁸ showed that regulating UBA2 (ubiquitin like modifier activating enzyme 2) expression inhibits the proliferation and migration of breast cancer cells and activates apoptosis. In our study, we investigated the apoptosis-mediated effects of monensin in SH-SY5Y cells by TUNEL, Annexin V, RT-PCR, and Western blot methods to answer the question of how monensin reduces cell viability in SH-SY5Y cells. In the present study, for the first time, it was shown and confirmed by different methods that monensin triggered apoptosis in SH-SY5Y cells in vitro. The TUNEL results of our study showed that the rate of apoptotic cells in the 8, 16, and 32 μM monensin applied groups was 17–37 times higher compared to the control group. In addition, Annexin V results showed that monensin administration increased the apoptosis of SH-SY5Y cells. Compared with the control group, 8, 16, and 32 μM monensin administration resulted in 9, 29, and 62-fold increases, respectively. The apoptosis profile shows that monensin effectively induces apoptosis at 8 and 16 μM doses in the early apoptotic period and at 32 μM in both early and late stages. In addition, Annexin V results support the TUNEL evaluation results. RT-PCR results showed that 8 μM monensin application caused apoptosis by increasing caspase-3, caspase-7, DR5, BMF, and BAD expressions, and decreasing caspase-9 expression. Besides, 16 μM monensin caused apoptosis by increasing caspase-7, MCL1, NOXA, and BCLAF expressions, and 32 μM monensin caused apoptosis by increasing caspase-3 and NOXA expressions and decreasing the caspase-9 expression. In addition, Western blot results showed that the monensin group triggered apoptosis by increasing caspase-3, 7, 8, and 9, and cleaved-PARP1 expressions and decreasing Bax and Bcl-2 expressions. Apoptosis is an essential regulator of tumor development and response to therapy.²⁶ Caspases are important in regulating apoptosis and are cysteine protease family

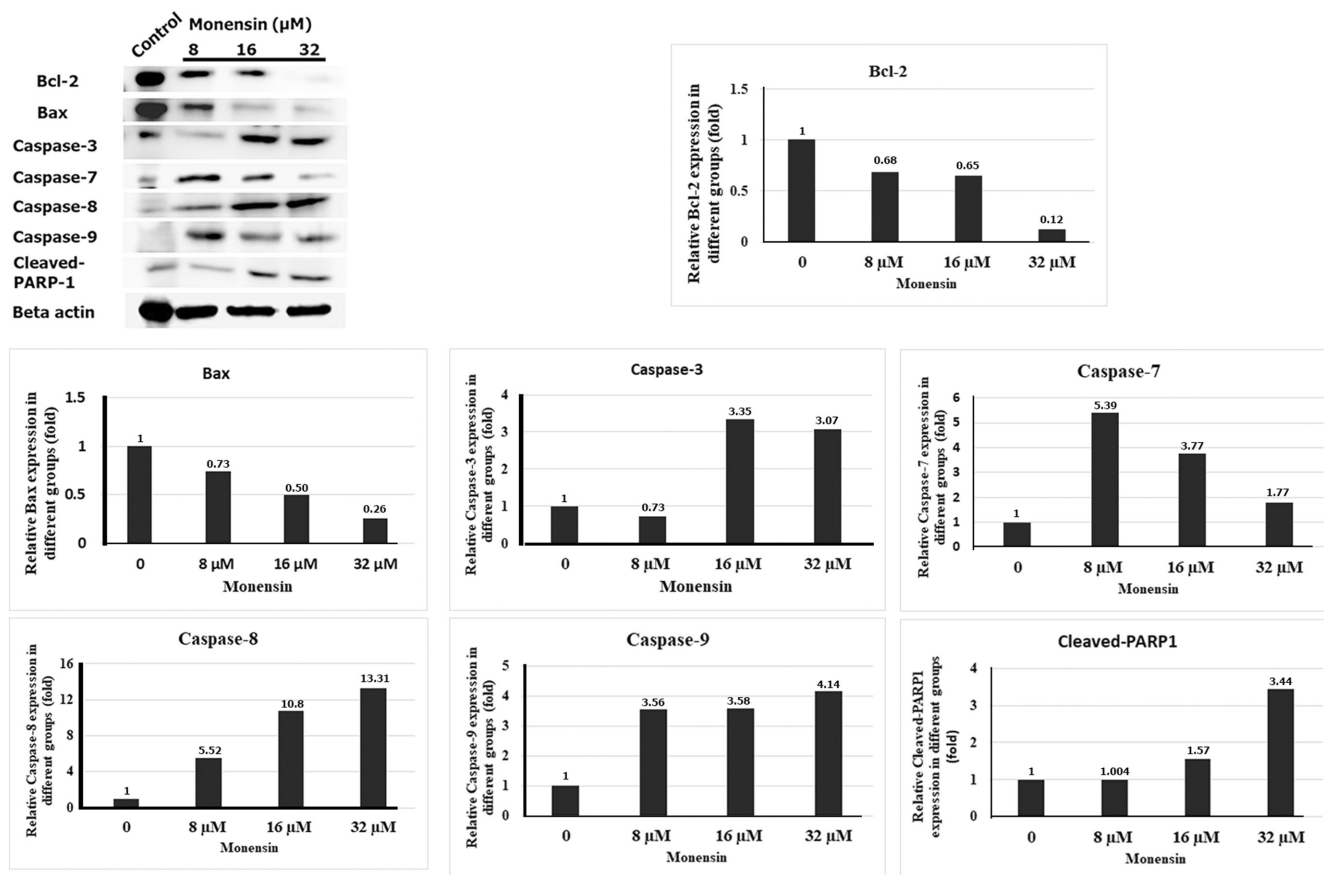


FIGURE 7 Evaluation of the effects of monensin on apoptosis in SH-SY5Y cells by Western blot.

members.²⁷ Caspase protease family members are essential in the initiation and maintenance of apoptosis. Whereas caspase-2, -8, -9, and 10 are essential regulators in the initiation of apoptosis, caspase-3, -6, and -7 play roles in the maintenance of apoptosis. Avoidance of apoptosis is the hallmark of cancer. Therefore, most current treatment modalities target caspase pathways to kill cancer cells and activate apoptosis signaling pathways.²⁸ Caspase-8 and caspase-10 have well-established roles in activating the extrinsic pathway, and caspase-9 is the critical enzyme for the intrinsic/mitochondrial pathway.²⁹ It is known that caspase 9 is involved in apoptosis as an initiator caspase and caspases 3 and 7 as effector caspases. Caspase-9 is activated by the release of cytochrome-c and functions to activate effector caspases and Bid. to remodel mitochondria. However, cell death is more effective in the presence of caspase 3, which is the primary stimulus of apoptosis. Caspase 7 does not contribute to intrinsic apoptosis susceptibility but can cause ROS production. This is related to caspase 7 in the effector role in the execution phase of apoptosis.³⁰ Our results show that monensin may have triggered apoptosis in SH-SY5Y cells by using caspase-8 and 9 as initiator caspases and caspase-3 and 7 as effector caspases. In addition, apoptosis in monensin-treated SH-SY5Y cells was accompanied with

the downregulation of Bcl-2 protein, supporting the idea that alteration of Bcl-2 is directly or indirectly involved in the apoptotic effect of monensin in SH-SY5Y cells. It has been suggested that a high ratio of Bax to Bcl-2 can cause the collapse of mitochondrial transmembrane potential, resulting in releasing cytochrome c and apoptosis.³¹ Park et al. showed that monensin induces apoptosis in NCI-H929 multiple myeloma cells through loss of mitochondrial transmembrane potential.³¹ Cytochrome C in the cytosol activates caspase-9 by forming an apoptosome. Caspase-9 activates procaspases to continue the apoptosis process. Many agents convert caspase-3 from inactive precursors to active enzymes during apoptosis. Similarly, our data report that monensin activates caspase-3 and impaired PARP protein. Monensin, a monocarboxylic Na⁺-ionophore antibiotic, arrests the cell cycle and is associated with loss of mitochondria transmembrane potential in renal cell carcinoma and many other cell lines.^{25,31-33} Monensin has been shown to decrease the mitochondrial transmembrane potential in renal cell carcinoma cells by TMRM and FACS staining.³² Therefore, monensin is able to trigger apoptosis by reduce the mitochondrial transmembrane potential in neuroblastoma cells as well as cell cause swelling, and cell cavitation because it is able to transport metal cations through membranes.

The limitations of this study are that monensin did not show its effect on nontumor cells and the reference drug was not used.

CONCLUSION

In conclusion, in our study, it has been shown that monensin decreases cell viability by triggering apoptosis-related mechanisms in SH-SY5Y neuroblastoma cells and also inhibits cell migration, invasion, and colony formation. Considering the features of monensin, which is the polyether ionophore investigated in our study, such as having a clean background profile in animal experiments (accelerating the development in the subjects, increasing milk production, and, most importantly, not causing any side effects), monensin is thought to be an agent that causes SH-SY5Y cell death through apoptotic factors.

AUTHOR CONTRIBUTIONS

F.B.S. and S.S.K. wrote the manuscript; S.S.K. designed the research; M.S. and C.O. performed the research; S.S.K., C.O. and M.S. analyzed the data; C.O. and M.S. contributed new reagents/analytical tools.

FUNDING INFORMATION

This study was supported by a grant from the Scientific and Technological Research Council of Turkey (TUBITAK-SBAG-120S399). This article will be published open access as per the agreement between TUBITAK ULAKBIM and Wiley.

CONFLICT OF INTEREST STATEMENT

The author(s) declared no potential conflicts of interest to the research, authorship, and/or publication of this article.

DATA AVAILABILITY STATEMENT

The data that support the findings of this study are available on request from the corresponding author.

ORCID

Sema Sertter Kocoglu  <https://orcid.org/0000-0002-3180-4007>

Ceren Oy  <https://orcid.org/0000-0002-2828-1196>

Mücahit Secme  <https://orcid.org/0000-0002-2084-760X>

F. Bahar Sunay  <https://orcid.org/0000-0002-2231-7979>

REFERENCES

- Mahapatra S, Challagundla KB. Neuroblastoma. StatPearls; 2022.
- Brodeur GM. Neuroblastoma: biological insights into a clinical enigma. *Nat Rev Cancer*. 2003;3:203-216.
- Maris JM. Recent advances in neuroblastoma. *N Engl J Med*. 2010;362:2202-2211.
- Radic-Sarikas B, Halasz M, Huber KVM, et al. Lapatinib potentiates cytotoxicity of YM155 in neuroblastoma via inhibition of the ABCB1 efflux transporter. *Sci Rep*. 2017;7:1-8.
- Vella S, Penna I, Longo L, et al. Perhexiline maleate enhances antitumor efficacy of cisplatin in neuroblastoma by inducing over-expression of NDM29 ncRNA. *Sci Rep*. 2015;5:1-13.
- Alexander F. Neuroblastoma. *Urol Clin North Am*. 2000;27:383-392.
- DuBois SG, Kalika Y, Lukens JN, et al. Metastatic sites in stage IV and IVS neuroblastoma correlate with age, tumor biology, and survival. *J Pediatr Hematol Oncol*. 1999;21:181-189.
- George SL, Parmar V, Lorenzi F, et al. Novel therapeutic strategies targeting telomere maintenance mechanisms in high-risk neuroblastoma. *J Exp Clin Cancer Res*. 2020;39:78.
- Ishola TA, Chung DH. Neuroblastoma. *Surg Oncol*. 2007;16:149-156.
- Olshan AF, De Roos AJ, Teschke K, et al. Neuroblastoma and parental occupation. *Cancer Causes Control*. 1999;10:539-549.
- Matthay KK, Maris JM, Schleiermacher G, et al. Neuroblastoma. *Nat Rev Dis Prim*. 2016;2:16078.
- Antoszczak M, Klejborowska G, Kruszyk M, Maj E, Wietrzyk J, Huczyński A. Synthesis and antiproliferative activity of silybin conjugates with salinomycin and monensin. *Chem Biol Drug des*. 2015;86(6):1378-1386.
- Markowska A, Kaysiewicz J, Markowska J, Huczyński A. Doxycycline, salinomycin, monensin and ivermectin repositioned as cancer drugs. *Bioorganic Med Chem Lett*. 2019;29:1549-1554.
- Tumova L, Pombinho AR, Vojtechova M, et al. Monensin inhibits canonical Wnt signaling in human colorectal cancer cells and suppresses tumor growth in multiple intestinal neoplasia mice. *Mol Cancer Ther*. 2014;13(4):812-822.
- Ketola K, Vainio P, Fey V, Kallioniemi O, Iljin K. Monensin is a potent inducer of oxidative stress and inhibitor of androgen signaling leading to apoptosis in prostate cancer cells. *Mol Cancer Ther*. 2010;12:3175-3185.
- Choi HS, Jeong E-H, Lee T-G, Kim SY, Kim H-R, Kim CH. Autophagy inhibition with monensin enhances cell cycle arrest and apoptosis induced by mTOR or epidermal growth factor receptor inhibitors in lung cancer cells. *Tuberc Respir Dis (Seoul)*. 2013;75:9-17.
- Wang X, Wu X, Zhang Z, et al. Monensin inhibits cell proliferation and tumor growth of chemo-resistant pancreatic cancer cells by targeting the EGFR signaling pathway. *Sci Rep*. 2018;8:1-15.
- Gu J, Huang L, Zhang Y. Monensin inhibits proliferation, migration, and promotes apoptosis of breast cancer cells via downregulating UBA2. *Drug Dev Res*. 2020;81:745-753.
- Esposito MR, Aveic S, Seydel A, Tonini GP. Neuroblastoma treatment in the post-genomic era. *J Biomed Sci*. 2017;24:14.
- Paraboschi I, Privitera L, Kramer-Marek G, Anderson J, Giuliani S. Novel treatments and technologies applied to the cure of neuroblastoma. *Children*. 2021;8:482.
- Zafar A, Wang W, Liu G, et al. Molecular targeting therapies for neuroblastoma: progress and challenges. *Med Res Rev*. 2021;41:961-1021.
- Rajendran V, Ilamathi HS, Dutt Lakshminarayana TS, Ghosh PC. Chemotherapeutic potential of monensin as an antimicrobial agent. *Curr Top Med Chem*. 2018;18:1976-1986.
- Verma SP, Das P. Monensin induces cell death by autophagy and inhibits matrix metalloproteinase 7 (MMP7) in UOK146 renal cell carcinoma cell line. *Vitr Cell Dev Biol - Anim*. 2018;54:736-742.

24. Kim SH, Kim KY, Yu SN, et al. Monensin induces PC-3 prostate cancer cell apoptosis via ROS production and Ca²⁺ homeostasis disruption. *Anticancer Res.* 2016;36:5835-5843.
25. Park WH, Seol JG, Kim ES, et al. Monensin-mediated growth inhibition in human lymphoma cells through cell cycle arrest and apoptosis. *Br J Haematol.* 2002;119:400-407.
26. Fulda S, Debatin KM. Extrinsic versus intrinsic apoptosis pathways in anticancer chemotherapy. *Oncogene.* 2006;25:4798-4811.
27. Degterev A, Boyce M, Yuan J. A decade of caspases. *Oncogene.* 2003;22:8543-8567.
28. Boice A, Bouchier-Hayes L. Targeting apoptotic caspases in cancer. *Biochim Biophys Acta – Mol Cell Res.* 2020;1867(6): 118688.
29. Picco R, Tomasella A, Fogolari F, Brancolini C. Transcriptomic analysis unveils correlations between regulative apoptotic caspases and genes of cholesterol homeostasis in human brain. *PLoS One.* 2014;9:e110610.
30. Brentnall MB, Rodriguez-Menocal L, De Guevara CE, Boise LH. Caspase-9, caspase-3 and caspase-7 have distinct roles during intrinsic apoptosis. *BMC Cell Biol.* 2013;14:32.
31. Park WH, Kim ES, Kim BK, Lee Y. Monensin-mediated growth inhibition in NCI-H929 myeloma cells via cell cycle arrest and apoptosis. *Int J Oncol.* 2003;23:197-204.
32. Park WH, Jung CW, Park JO, et al. Monensin inhibits the growth of renal cell carcinoma cells via cell cycle arrest or apoptosis. *Int J Oncol.* 2003;22:855-860.
33. Park WH, Lee MS, Park K, Kim ES, Kim BK, Lee YY. Monensin-mediated growth inhibition in acute myelogenous leukemia cells via cell cycle arrest and apoptosis. *Int J Cancer.* 2002;101:235-242.

SUPPORTING INFORMATION

Additional supporting information can be found online in the Supporting Information section at the end of this article.

How to cite this article: Serter Kocoglu S, Oy C, Secme M, Sunay FB. Investigation of the anticancer mechanism of monensin via apoptosis-related factors in SH-SY5Y neuroblastoma cells. *Clin Transl Sci.* 2023;16:1725-1735. doi:[10.1111/cts.13593](https://doi.org/10.1111/cts.13593)